Chemical Science

ROYAL SOCIETY OF CHEMISTRY

EDGE ARTICLE

View Article Online
View Journal | View Issue

Cite this: *Chem. Sci.*, 2020, **11**, 1097

All publication charges for this article have been paid for by the Royal Society of Chemistry

Received 12th November 2019
Accepted 4th December 2019

DOI: 10.1039/c9sc05728e

rsc.li/chemical-science

Reversible reduction drives anion ejection and C_{60} binding within an $Fe^{II}_4L_6$ cage†

Zhenpin Lu, Tanya K. Ronson and Jonathan R. Nitschke *

$Fe^{II}_4L_6$ tetrahedral cage **1** was prepared from a redox-active dicationic naphthalenediimide (NDI) ligand. The +20 charge of the cage makes it a good host for anionic guests, with no binding observed for neutral aromatic molecules. Following reduction by Cp_2Co, the cage released anionic guests; subsequent oxidation by $AgNTf_2$ led to re-uptake of anions. In its reduced form, however, **1** was observed to bind neutral C_{60}. The fullerene guest was subsequently ejected following cage re-oxidation. The guest release process was found to be facilitated by anion-mediated transport from organic to aqueous solution. Cage **1** thus employs electron transfer as a stimulus to control the uptake and release of both neutral and charged guests, through distinct pathways.

Introduction

Self-assembled metal–organic cages[1] have found uses across various fields, ranging from chemical separations,[2] catalyzing organic reactions,[3] sensing specific analytes[4] and acting as photoreactors,[5] among others. These applications are often based on encapsulation of guests within the well-defined inner cavities of cages. Guest uptake and release by a host molecule can be controlled using stimuli such as heat,[6] light,[7] pH[8] and competing guests,[9] as understanding has increased as to how to design stimuli-responsive behaviour.[10] The use of redox stimuli is particularly attractive[11] because electrons are 'clean' stimuli, producing no chemical by-products. Thus far, several redox-active metal–organic cages have been successfully synthesized.[11c] Recently Sallé, Goeb and co-workers reported several tetrathiafulvalene based coordination cages, which can reversibly uptake and release perfluorocarborate[11d] or corronene[11a] guests under redox control. Inspired by these achievements, we sought to develop new redox-active metal–organic cage systems capable of reversible guest uptake. In the present system, electron transfer was used to stimulate the uptake and release of both anionic and neutral guests, *via* distinct pathways.

Naphthalenediimides (NDIs) and their derivatives are redox-active electron-deficient compounds, and can be readily substituted with a wide variety of functional groups,[12] making them ideal building blocks for metal–organic cages.[13] We have reported several NDI-diamine based tetrahedral metal–organic cages, with the redox behaviour of one catalyzing the oxidative coupling of arylborates to give biphenyls.[14] However, reduction of that cage[14] resulted in precipitation due to charge neutralization. This behaviour prevented further study of its redox dependent host–guest chemistry in solution. In order to solve this issue, we designed a new dicationic subcomponent, **A** (Fig. 1). We hypothesised that the permanent charges of **A**

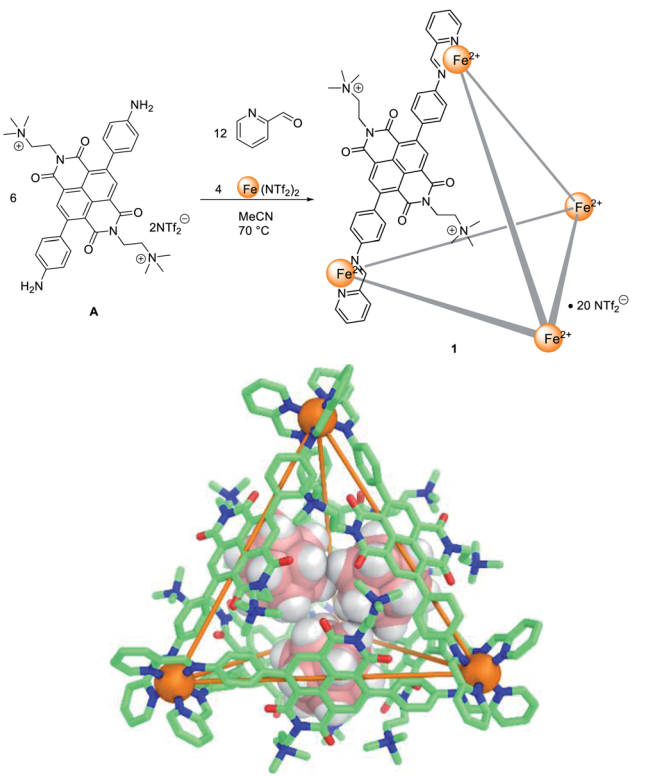

Fig. 1 The synthesis of $Fe^{II}_4L_6$ cage **1** (top) and crystal structure of **1** with three carborate anions encapsulated (bottom). Cage hydrogen atoms, counterions, solvents and disorder are omitted for clarity.

Department of Chemistry, University of Cambridge, Lensfield Road, Cambridge CB2 1EW, UK. E-mail: jrn34@cam.ac.uk

† Electronic supplementary information (ESI) available. CCDC 1935513. For ESI and crystallographic data in CIF or other electronic format see DOI: 10.1039/c9sc05728e

would improve the solubility of the corresponding cage **1**, following reduction of the NDI moieties. This $Fe^{II}_4L_6$ cage, **1**, did indeed remain in solution upon NDI reduction, enabling different guests to be taken up and released upon reduction and oxidation of the cage.

Results and discussion

Tetrahedral $Fe^{II}_4L_6$ cage **1** was synthesized from quaternary-ammonium-functionalized NDI subcomponent **A** (6 equiv.), 2-formylpyridine (12 equiv.) and $Fe(NTf_2)_2$ (4 equiv.) in acetonitrile (Fig. 1). The ^{1}H NMR spectrum of **1** was consistent with a single symmetric species (Fig. S2–S7†). ESI-MS of **1** confirmed the formation of an assembly with $Fe^{II}_4L_6$ stoichiometry (Fig. S8–S11†). Subcomponent **A** was not observed to form the Zn_4L_6 analogue of **1** when $Zn(NTf_2)_2$ was used in place of the iron salt. We infer this lack of reactivity to be due to the weaker metal–ligand bonds involving zinc not being able to compensate for coulombic repulsion among the cationic ligands.

Single crystals of **1** were obtained from vapour diffusion of diisopropyl ether into an acetonitrile solution of **1** containing cesium carborane (10 equiv.). The crystal structure of **1** revealed a *T*-symmetric framework (Fig. 1), with six ligands bridging four octahedral iron(II) centres of the same handedness. The solid state structure is consistent with NMR data, in which all ligands are magnetically equivalent. The metal–metal distances are in the range 18.771(3)–19.345(2) Å (average 19.1 Å). The NDI moieties lie tangent to the edges of the tetrahedron, affording an enclosed cavity which is further blocked by the $-(CH_2)_2N^+(Me)_3$ substituents of the ligands. A cavity volume of 1100 Å^3 was determined using VOIDOO[15] (Fig. S26†). Three carborate anions were found in the cavity in the solid state.

The electrochemical properties of cage **1** and subcomponent **A** were investigated by cyclic voltammetry, carried out in 0.1 M ^{n}Bu$_4$N$^+$Tf$_2$N$^-$ in MeCN at a scan rate of 500 mV s^{-1}. Similar to other NDI derivatives,[14,16] cage **1** exhibited a quasi-reversible process upon reduction (Fig. 2), in which the first reduction wave appeared at −0.81 V *vs.* Fc/Fc* and the second occurred at −1.19 V. The related oxidation waves were found at −1.29 and −0.78 V. Reduction was reversible over several cycles. In comparison, two similar reduction waves (at −0.96 and −1.36 V) were also observed for subcomponent **A** (Fig. S25†). However, the intensity of the CV signals decreased with each cycle in the case of **A**, consistent with irreversible reactions following redox events for **A**, but not for **1**. We thus infer that self-assembly rendered the NDI panels more robust to redox processes.

In light of our electrochemical studies, we investigated the reactions of **1** with chemical reductants and oxidants. Cp_2Co and $AgNTf_2$ were selected as an appropriate one-electron reductant and oxidant, respectively, for **1**. Following the addition of Cp_2Co (10 equiv.), a sharp signal attributed to Cp_2Co^+ appeared at 5.67 ppm in the ^{1}H NMR spectrum, indicating that cage reduction had occurred. Following reduction, the cage signals became NMR silent due to the formation of radical species, as was observed previously in the case of related systems.[14,17] When $AgNTf_2$ (12 equiv.) was added to the mixture, the cage signals reappeared cleanly (Fig. S41†), demonstrating the reversibility of the process.

Next we investigated the binding behaviour of **1** with various prospective guests using ^{1}H NMR spectroscopy in CD_3CN. Cage **1** did not show measurable affinity towards the neutral species investigated (Fig. 3 and S27–S32†) despite the enclosed cavity observed in the crystal structure (Fig. 1).

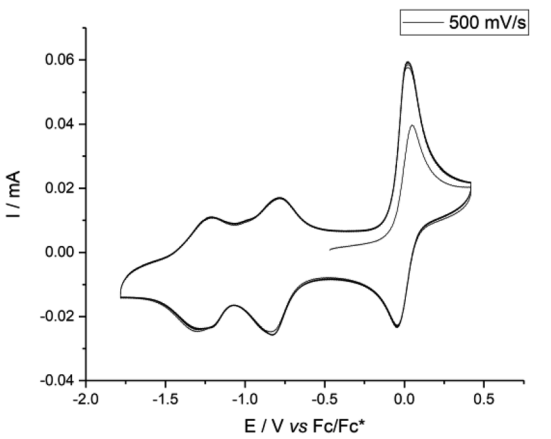

Fig. 2 Cyclic voltammetry (5 scans, 500 mV s^{-1}) of **1** in MeCN (0.1 M ^{n}Bu$_4$N$^+$Tf$_2$N$^-$) at 25 °C.

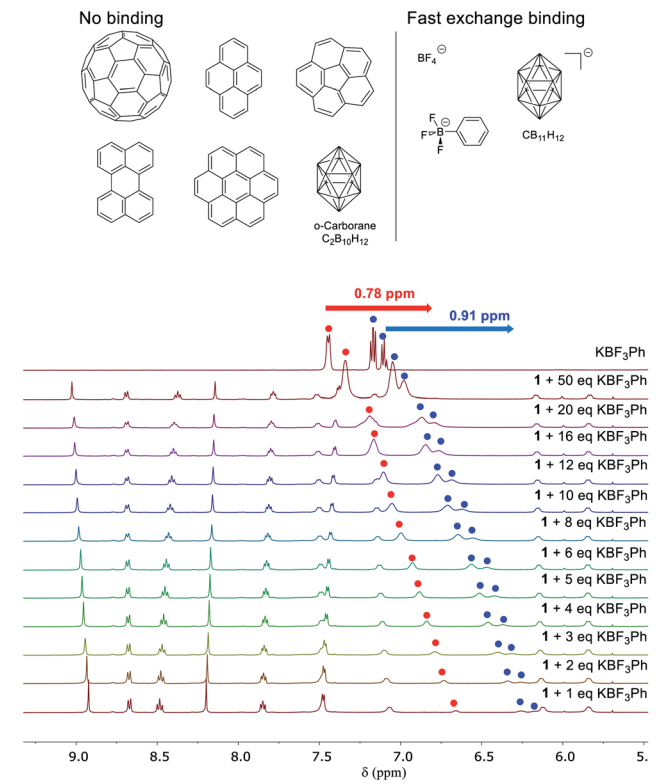

Fig. 3 Top, neutral aromatic non-guests and anionic guests for cage **1**; bottom, a stacked plot of the ^{1}H NMR titration (500 MHz, 298 K) of KBF_3Ph into a solution of **1** (0.17 mM) in CD_3CN. The signals from the guest (KBF_3Ph) have been labelled with red and blue dots, and the others belong to cage **1**.

Only the anions BF_4^-, $PhBF_3^-$ and $CB_{11}H_{12}^-$ were observed to bind in fast exchange on the NMR chemical-shift timescale (Fig. 3 and S33–S40†). For instance, the ^{1}H NMR signals of $PhBF_3^-$ were shifted upfield by up to 0.91 ppm in the presence of **1**. Similar chemical shift changes were also observed in the ^{19}F NMR spectrum of this anion (Fig. S37†); host signals were also observed to shift in the presence of guests. However, the binding stoichiometries of these anions in cage **1** could not be established due to their fast exchange binding, and attempts to crystallize these host–guest adducts were also not successful. The ^{19}F NMR signal of triflimide shifted upon the addition of KBF_3Ph, suggesting that the encapsulated Tf_2N^- anions were released in the presence of the competing guest $PhBF_3^-$ (Fig. S36†). We infer the cationic nature of subcomponent **A** to impart the cage with a higher binding affinity for anionic guests relative to neutral guests.

$PhBF_3^-$ was chosen as a model guest to probe the binding behaviour of **1** under redox control. During the stepwise addition of Cp_2Co, the ^{1}H NMR signals of $PhBF_3^-$ gradually shifted downfield, towards the values for the free guest (Fig. 4).

We infer the reduction of the NDI panels of **1** to result in repulsion between the anionic guest and the reduced cage panels, leading to release of the bound guests. The signals of **1** broadened into the baseline during the reduction process due to the formation of radical anion species. After the addition of 10 equivalents of Cp_2Co, the ^{1}H NMR signals of $PhBF_3^-$ were found at the same chemical shift values as the free anion, suggesting complete ejection of the guest from the cage cavity. Full recovery of the ^{1}H NMR spectrum of $PhBF_3^- \subset$ **1** was observed after the addition of $AgNTf_2$ (12 equiv.).

We next investigated the use of electron transfer to control the uptake and release and of neutral molecules. Although cage **1** possesses a +20 charge, which favours the binding of anions, we reasoned that reduction of the NDI panels with Cp_2Co would partially neutralize the charge and potentially modify the guest preference.

The X-ray structure of **1** (Fig. 1) suggested that cage **1** would have a suitable volume (Fig. S26†) to accommodate C_{60}, and analogous cages have been shown to bind fullerenes well.[14,18] C_{60} thus appeared to be an ideal guest molecule to test the catch-and-release cycle shown in Fig. 5. This cycle is inferred to have three distinct stages. First, after the addition of Cp_2Co, reduced cage **1** released the anionic guest in favour of neutral C_{60}. Second, treatment with $AgNTf_2$ oxidized the cage back to its initial state, giving $C_{60} \subset$ **1** as a kinetically-trapped species. Third, the thermodynamically-unfavourable $C_{60} \subset$ **1** released neutral C_{60}, generating the more stable triflimide adduct.

To test the cycle of Fig. 5, a solution of reduced cage **1**, prepared through addition of Cp_2Co (10 equiv.) to **1** in CD_3CN, was mixed with C_{60} (4 equiv.), and the mixture was kept at room temperature overnight. $AgNTf_2$ (12 equiv.) was added to oxidize the cage back to its initial state. The presence of C_{60} was confirmed by ^{13}C NMR (Fig. S15 and S21†) in CD_3CN, a solvent in which free C_{60} displays negligible solubility.[19]

Cage **1** exhibited *T* point symmetry in solution, as reflected in its ^{1}H NMR spectra,[20] however, the encapsulation of C_{60} within **1** resulted in the formation of diastereomers having all possible combinations of Δ and Λ metal stereochemistries with *T*, S_4,

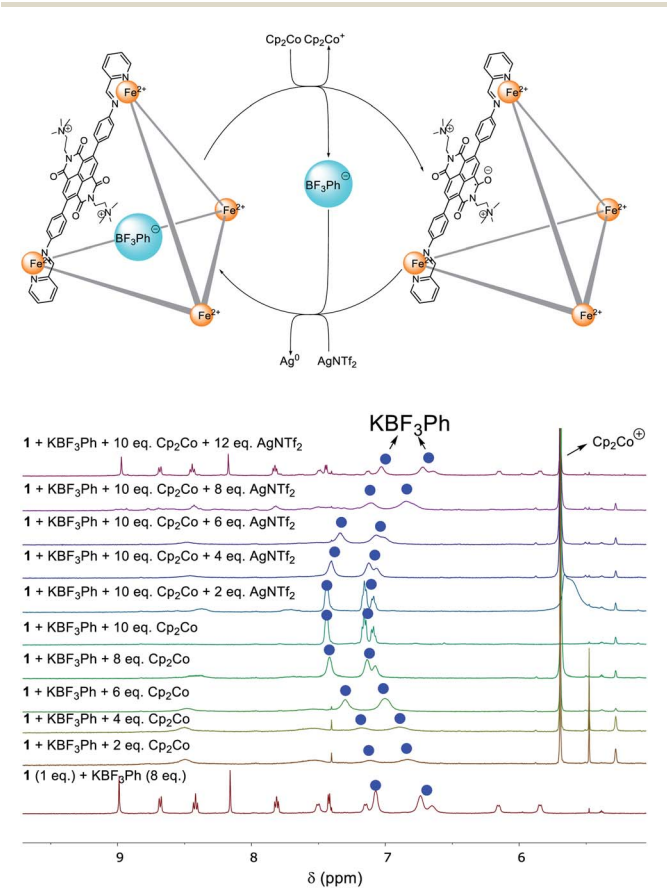

Fig. 4 Redox control of KBF_3Ph binding within **1**.

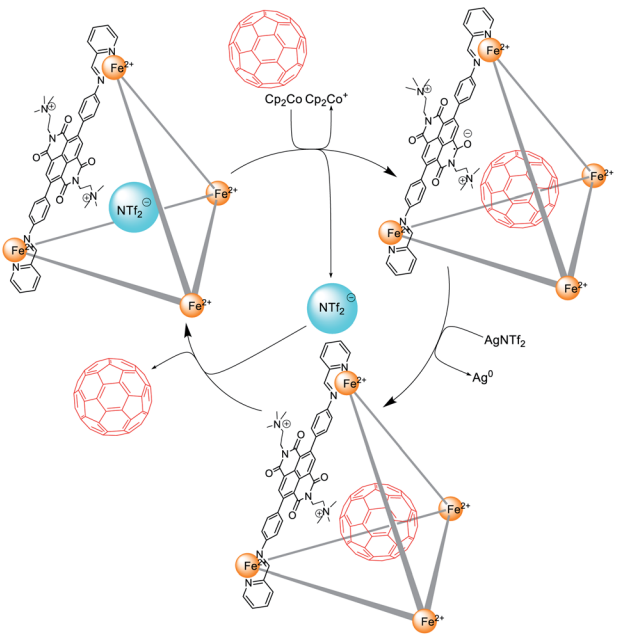

Fig. 5 The encapsulation and release of C_{60} within cage **1** following reduction and subsequent re-oxidation.

and C_3 point symmetries (Fig. S13†).[13d,20] Interestingly, the $C_{60} \subset$ **1** complex was found to be a kinetically trapped species. After 5 days the S_4 and C_3 diastereomers[20] (Fig. S19†) of $C_{60} \subset$ **1** released their encapsulated C_{60} with concomitant formation of free **1** and a reduction in the intensity of ^{13}C NMR signal for C_{60} (Fig. S21†). Only the *T* diastereomer[20] of $C_{60} \subset$ **1** (14% by ^{1}H NMR integration) remained in solution after 30 days, indicating its greater kinetic stability relative to the other diastereomers of $C_{60} \subset$ **1** (Fig. 6).

Counteranions have been shown to drive the phase transfer of cationic coordination cages, permitting guests to be conveyed across phase boundaries.[1a,1c] The treatment of a solution of cage **1** in MeCN/EtOAc (1 : 1) with aqueous Na_2SO_4 resulted in transfer of **1** from the organic phase into water (Fig. S42 and S43†) as the sulfate salt.[1a] Treatment with aqueous Na_2SO_4 likewise stimulated phase transfer of the $C_{60} \subset$ **1** host–guest complex. This complex, however, was observed to release C_{60} upon phase transfer, allowing cargo recovery by filtration (Fig. 7, S44 and S45†). This novel use of phase transfer to effect guest ejection could enable new means of chemical purification, whereby a guest is separated from its recyclable host in a single step, rather than requiring a separate purification step.[21]

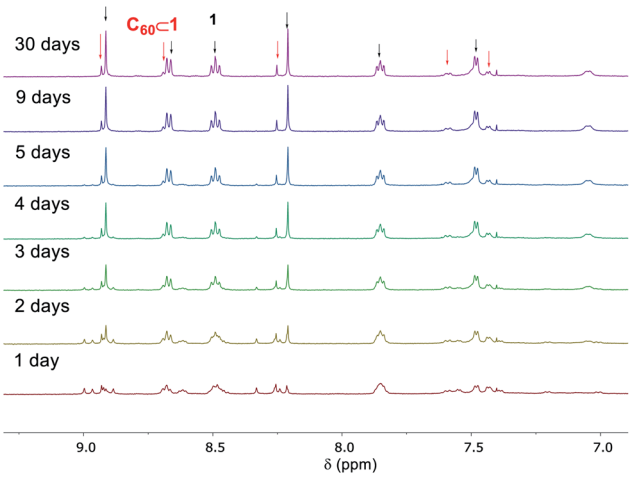

Fig. 6 The release of C_{60} from $C_{60} \subset$ **1** monitored by ^{1}H NMR (500 MHz, CD_3CN) over the course of a month.

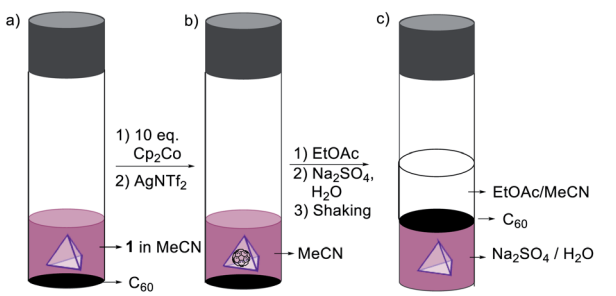

Fig. 7 (a) Mixture of cage **1** and C_{60} in MeCN. (b) Formation of $C_{60} \subset$ **1**. (c) The release of C_{60} and transfer of cage **1** from the EtOAc/MeCN to the water layer.

Conclusions

In this study, we reported a new redox-switchable $Fe^{II}_4L_6$-tetrahedral cage. Although, the cage shows binding affinity for anionic guests, following reduction the cage was observed to encapsulate neutral C_{60} with ejection of the anionic guests. Current efforts are focused on expanding redox-stimulated guest uptake and release to a broader set of guest species, and applying these concepts to design new systems where electrical energy may be used directly to effect chemical separations and transport.

Conflicts of interest

There are no conflicts to declare.

Acknowledgements

This work was supported by the European Research Council (695009) and the UK Engineering and Physical Sciences Research Council (EPSRC, EP/P027067/1 and EP/M008258/1). Z. L. thanks the Deutsche Forschungsgemeinschaft (DFG) for a Postdoctoral fellowship. We thank Diamond Light Source (UK) for synchrotron beamtime on I19 (MT15768).

Notes and references

1 (*a*) R. Chakrabarty, P. S. Mukherjee and P. J. Stang, *Chem. Rev.*, 2011, **111**, 6810–6918; (*b*) J. R. Nitschke, *Acc. Chem. Res.*, 2007, **40**, 103–112; (*c*) D. Samanta, S. Shanmugaraju, S. A. Joshi, Y. P. Patil, M. Nethajia and P. S. Mukherjee, *Chem. Commun.*, 2012, **48**, 2298–2300.

2 (*a*) A. B. Grommet and J. R. Nitschke, *J. Am. Chem. Soc.*, 2017, **139**, 2176–2179; (*b*) B. S. Pilgrim, D. A. Roberts, T. G. Lohr, T. K. Ronson and J. R. Nitschke, *Nat. Chem.*, 2017, **9**, 1276–1281; (*c*) A. B. Grommet, J. B. Hoffman, E. G. Percastegui, J. Mosquera, D. J. Howe, J. L. Bolliger and J. R. Nitschke, *J. Am. Chem. Soc.*, 2018, **140**, 14770–14776; (*d*) J. Lee, C. Y. Chuah, J. Kim, Y. Kim, N. Ko, Y. Seo, K. Kim, T. H. Bae and E. Lee, *Angew. Chem., Int. Ed.*, 2018, **57**, 7869–7873; (*e*) B. Roy, A. Kumar Ghosh, S. Srivastava, P. D'Silva and P. S. Mukherjee, *J. Am. Chem. Soc.*, 2015, **137**, 11916–11919.

3 (*a*) M. Yoshizawa, M. Tamura and M. Fujita, *Science*, 2006, **312**, 251–254; (*b*) P. L. Manna, C. Talotta, G. Floresta, M. De Rosa, A. Soriente, A. Rescifina, C. Gaeta and P. Neri, *Angew. Chem., Int. Ed.*, 2018, **57**, 5423–5428; (*c*) D. Preston, J. J. Sutton, K. C. Gordon and J. D. Crowley, *Angew. Chem., Int. Ed.*, 2018, **57**, 8659–8663; (*d*) W. Cullen, A. J. Metherell, A. B. Wragg, C. G. P. Taylor, N. H. Williams and M. D. Ward, *J. Am. Chem. Soc.*, 2018, **140**, 2821–2828.

4 (*a*) P. D. Frischmann, V. Kunz and F. Würthner, *Angew. Chem., Int. Ed.*, 2015, **54**, 7285–7289; (*b*) S. Shanmugaraju and P. S. Mukherjee, *Chem.–Eur. J.*, 2015, **21**, 6656–6666; (*c*) Q. Q. Wang, V. W. Day and K. Bowman-James, *J. Am. Chem. Soc.*, 2013, **135**, 392–399.

5 (*a*) M. Yoshizawa, Y. Takeyama, T. Kusukawa and M. Fujita, *Angew. Chem., Int. Ed.*, 2002, **41**, 1347–1349; (*b*) M. Yoshizawa, S. Miyagi, M. Kawano, K. Ishiguro and M. Fujita, *J. Am. Chem. Soc.*, 2004, **126**, 9172–9173; (*c*) T. Murase, S. Sato and M. Fujita, *Angew. Chem., Int. Ed.*, 2007, **46**, 5133–5136; (*d*) N. Kishi, M. Akita, M. Kamiya, S. Hayashi, H.-F. Hsu and M. Yoshizawa, *J. Am. Chem. Soc.*, 2013, **135**, 12976–12979.

6 (*a*) J. H. Tang, Y. Sun, Z. L. Gong, Z. Y. Li, Z. Zhou, H. Wang, X. Li, M. L. Saha, Y. W. Zhong and P. J. Stang, *J. Am. Chem. Soc.*, 2018, **140**, 7723–7729; (*b*) H. Wu, Y. Chen, L. Zhang, O. Anamimoghadam, D. Shen, Z. Liu, K. Cai, C. Pezzato, C. L. Stern, Y. Liu and J. F. Stoddart, *J. Am. Chem. Soc.*, 2019, **141**, 1280–1289.

7 (*a*) M. Han, R. Michel, B. He, Y. S. Chen, D. Stalke, M. John and G. H. Clever, *Angew. Chem., Int. Ed.*, 2013, **52**, 1319–1323; (*b*) S. E. Border, R. Z. Pavlovic, L. Zhiquan and J. D. Badjic, *J. Am. Chem. Soc.*, 2017, **139**, 18496–18499; (*c*) A. J. McConnell, C. J. E. Haynes, A. B. Grommet, C. M. Aitchison, J. Guilleme, S. Mikutis and J. R. Nitschke, *J. Am. Chem. Soc.*, 2018, **49**, 16952–16956; (*d*) F. C. Parks, Y. Liu, S. R. Stutsman, S. Debnath, K. Raghavachari and A. H. Flood, *J. Am. Chem. Soc.*, 2018, **140**, 17711–17723.

8 (*a*) K. Kurihara, K. Yazaki, M. Akita and M. Yoshizawa, *Angew. Chem., Int. Ed.*, 2017, **56**, 11360–11364; (*b*) W. Cullen, K. A. Thomas, C. A. Hunter and M. D. Ward, *Chem. Sci.*, 2015, **6**, 4025–4028; (*c*) X. Ji, Y. Yao, J. Li, X. Yan and F. Huang, *J. Am. Chem. Soc.*, 2013, **135**, 74–77; (*d*) I. A. Riddell, M. M. J. Smulders, J. K. Clegg and J. R. Nitschke, *Chem. Commun.*, 2011, **47**, 457–459; (*e*) X. Su, S. Voskian, R. P. Hughes and I. Aprahamian, *Angew. Chem., Int. Ed.*, 2013, **52**, 10734–10739.

9 (*a*) A. M. Castilla, T. K. Ronson and J. R. Nitschke, *J. Am. Chem. Soc.*, 2016, **138**, 2342–2351; (*b*) M. C. Young, L. R. Holloway, A. M. Johnson and R. J. Hooley, *Angew. Chem., Int. Ed.*, 2014, **53**, 9832–9836.

10 (*a*) T. Y. Kim, R. A. S. Vasdev, D. Preston and J. D. Crowley, *Chem.–Eur. J.*, 2018, **24**, 14878–14890; (*b*) A. Goswami, S. Saha, P. K. Biswas, and M. Schmittel, *Chem. Rev.*, DOI: 10.1021/acs.chemrev.9b00159; (*c*) W. Wang, Y. Wang and H. B. Yang, *Chem. Soc. Rev.*, 2016, **45**, 2656–2693; (*d*) M. Schmittel, *Chem. Commun.*, 2015, **51**, 14956–14968.

11 (*a*) G. Szalóki, V. Croué, V. Carré, F. Aubriet, O. Alévêque, E. Levillain, M. Allain, J. Aragó, E. Ortí, S. Goeb and M. Sallé, *Angew. Chem., Int. Ed.*, 2017, **56**, 16272–16276; (*b*) K. Yazaki, S. Noda, Y. Tanaka, Y. Sei, M. Akita and M. Yoshizawa, *Angew. Chem., Int. Ed.*, 2016, **55**, 15031–15034; (*c*) V. Croué, S. Goeb, G. Szalóki, M. Allain and M. Sallé, *Angew. Chem., Int. Ed.*, 2016, **55**, 1746–1750; (*d*) C. Colomban, G. Szalóki, M. Allain, L. Gómez, S. Goeb, M. Sallé, M. Costas and X. Ribas, *Chem.–Eur. J.*, 2017, **23**, 3016–3022; (*e*) Y. Satoh, L. Catti, M. Akita and M. Yoshizawa, *J. Am. Chem. Soc.*, 2019, **141**, 12268–12273; (*f*) K. Mahata, P. D. Frischmann and F. Würthner, *J. Am. Chem. Soc.*, 2013, **135**, 15656–15661.

12 M. A. Kobaisi, S. V. Bhosale, K. Latham, A. M. Raynor and S. V. Bhosale, *Chem. Rev.*, 2016, **116**, 11685–11796.

13 (*a*) Y. Wu, M. D. Krzyaniak, J. F. Stoddart and M. R. Wasielewski, *J. Am. Chem. Soc.*, 2017, **139**, 2948–2951; (*b*) S. P. Black, D. M. Wood, F. B. Schwarz, T. K. Ronson, J. J. Holstein, A. R. Stefankiewicz, C. A. Schalley, J. K. M. Sanders and J. R. Nitschke, *Chem. Sci.*, 2016, **7**, 2614–2620; (*c*) S. P. Black, A. R. Stefankiewicz, M. M. J. Smulders, D. Sattler, C. A. Schalley, J. R. Nitschke and J. K. M. Sanders, *Angew. Chem., Int. Ed.*, 2013, **52**, 5749–5752; (*d*) T. K. Ronson, D. A. Roberts, S. P. Black and J. R. Nitschke, *J. Am. Chem. Soc.*, 2015, **137**, 14502–14512.

14 Z. Lu, R. Lavendomme, O. Burghaus and J. R. Nitschke, *Angew. Chem., Int. Ed.*, 2019, **58**, 9073–9077.

15 G. J. Kleywegt and T. A. Jones, *Acta Crystallogr., Sect. D: Biol. Crystallogr.*, 1994, **50**, 178–185.

16 S. Suraru, C. Burschka and F. Würthner, *J. Org. Chem.*, 2014, **79**, 128–139.

17 G. Belanger-Chabot, A. Ali and F. P. Gabbaï, *Angew. Chem., Int. Ed.*, 2017, **56**, 9958–9961.

18 T. K. Ronson, W. Meng and J. R. Nitschke, *J. Am. Chem. Soc.*, 2017, **139**, 9698–9707.

19 K. N. Semenov, N. A. Charykov, V. A. Keskinov, A. K. Piartman, A. A. Blokhin and A. A. Kopyrin, *J. Chem. Eng. Data*, 2010, **55**, 13–36.

20 M_4L_6 cages are often found to present a mixture of three diastereomers, having distinct symmetries: homochiral *T*, with all metal centers having the same Δ or Λ configuration, heterochiral C_3, with ΔΔΔΛ/ΛΔΔΔ configuration, and achiral S_4, having ΔΔΛΛ metal center handednesses. See W. Meng, J. K. Clegg, J. D. Thoburn and J. R. Nitschke, *J. Am. Chem. Soc.*, 2011, **133**, 13652–13660.

21 D. Zhang, T. K. Ronson, J. Mosquera, A. Martinez and J. R. Nitschke, *Angew. Chem., Int. Ed.*, 2018, **57**, 3717–3721.